Uniting Low- and High-Sensitivity Experiments through Generalised NMR Supersequences

Jonathan R. J. Yong,[1] Ēriks Kupče,[2] Tim D. W. Claridge[1,*]

[1] *Chemistry Research Laboratory, Department of Chemistry, University of Oxford, Mansfield Road, Oxford, OX1 3TA, United Kingdom*

[2] *Bruker UK Ltd, R&D, Coventry CV4 9GH, United Kingdom*

[*] tim.claridge@chem.ox.ac.uk

---

https://www.rsc.org/journals-books-databases/about-journals/chemcomm#writing-guidelines

https://www.rsc.org/journals-books-databases/author-and-reviewer-hub/authors-information/prepare-and-format/

TODO: TOC graphic and TOC text (15–25 words)

Abstract

NOAH supersequences represent a time-efficient way of collecting multiple 2D NMR experiments. We show here that experiments with very different sensitivity requirements, including 1,1-ADEQUATE and HSQC, may be efficiently combined through interleaved supersequences, which assign each module a different number of transients and fully generalise the concept of parallel supersequences.

(50 words)

1 Introduction

Nuclear magnetic resonance (NMR) spectroscopy plays a key role in the structural elucidation of natural products; in particular, two-dimensional (2D) NMR experiments provide vast amounts of information on through-bond and through-space molecular connectivity.[1,2] However, these experiments are often time-consuming as they require the incrementation of indirect-dimension evolution periods in order to construct the requisite 2D data matrices. One particularly flexible method for accelerating 2D data acquisition is the NOAH (NMR by Ordered Acquisition using ^{1}H detection) technique,[3,4] in which multiple 2D experiments ('modules') are combined into a single experiment using only a single recovery delay. These nested 'supersequences', which rely on the tailored excitation of magnetisation from different sources, provide an array of 2D spectra (up to 10 so far) in greatly reduced experiment times.

Virtually all common 2D experiments, such as HSQC, HMQC, COSY, TOCSY, and NOESY, have been implemented in NOAH supersequences, allowing for the (manual or computer-assisted) structural eluci-

dation of a wide range of molecules.[5–7] However, such experiments tend to fall short in proton-sparse molecules[8–10] as they do not yield sufficient correlations. In such cases, additional information may be obtained through the HMBC[11–13] and HSQMBC[14–16] experiments which detect long-range X–^{1}H couplings ($^{n}J_{XH}$, X = ^{13}C or ^{15}N). Although these tend to yield vastly more correlations, there often remains ambiguity in interpreting the resulting data as these techniques do not reveal the exact number of bonds over which a coupling is mediated. In contrast, one-bond ^{13}C–^{13}C correlations ($^{1}J_{CC}$), obtained through the INADEQUATE[17]—or more practically, ADEQUATE[18,19]—experiments, allow chemists to directly trace out carbon- and nitrogen-containing backbones with much greater certainty. The main limitation of such experiments is their low sensitivity, as they rely on pairs of heteronuclei with low natural abundances; nonetheless, with the introduction of cryogenically cooled probes and concomitant advances in achievable signal-to-noise ratios (SNRs), such experiments can nowadays be feasibly run even on dilute samples.

To date, insensitive experiments such as ^{15}N HMBC and ADEQUATE have not been the main focus of NOAH supersequences.[20] This is because in a traditional 'linear' supersequence, each constituent module is recorded with the same number of transients. The total experiment duration is therefore dictated by the module with the lowest sensitivity, and higher-sensitivity modules (e.g. HSQC or COSY) would be recorded with far more transients than would be necessary. Although the more sensitive modules would still be obtained 'for free', the *effective* time savings thus realised would be far smaller than for a supersequence constructed from modules with balanced sensitivities.

For this reason, the low-sensitivity ADEQUATE and ^{15}N HMBC modules form a 'natural' pairing in the NOAH-2 AB_N supersequence introduced here (Figure 1b). However, in this work, we also go beyond the traditional 'linear' or 'horizontal' model of a supersequence in adding more modules through 'vertical' interleaving, in a similar fashion to the parallel supersequences recently described.[7] We show that, following an initial ADEQUATE module, up to four modules (^{15}N HMBC, ^{13}C HMBC, ^{15}N sensitivity-enhanced HSQC (seHSQC), and ^{13}C HSQC) may be interleaved in this 'vertical' fashion (Figures 1d and 1e), yielding five modules with balanced intensities and high-quality data. By tailoring the number of times each module is acquired, this technique provides a powerful and flexible way to balance modules with different sensitivities, and fully generalises our previous work on parallel supersequences, where only two modules were interleaved at a time.

2 NOAH-2 AB_N

When designing NMR supersequences, it is generally a good rule of thumb to place the module with the lowest sensitivity first: this is because any incomplete preservation of magnetisation by earlier modules will lead to decreased sensitivity in later modules. The 1,1-ADEQUATE module, which relies on neighbouring pairs of ^{13}C nuclei—occurring only in roughly 1 out of 8130 molecules—therefore forms the beginning of all the supersequences described here.

The ADEQUATE module (Figure 1a) is designed to only use the magnetisation of protons directly bonded to ^{13}C, which we denote here as $^{1}H^{C}$.[22,23] In order to maintain the sensitivity of later modules, it must return

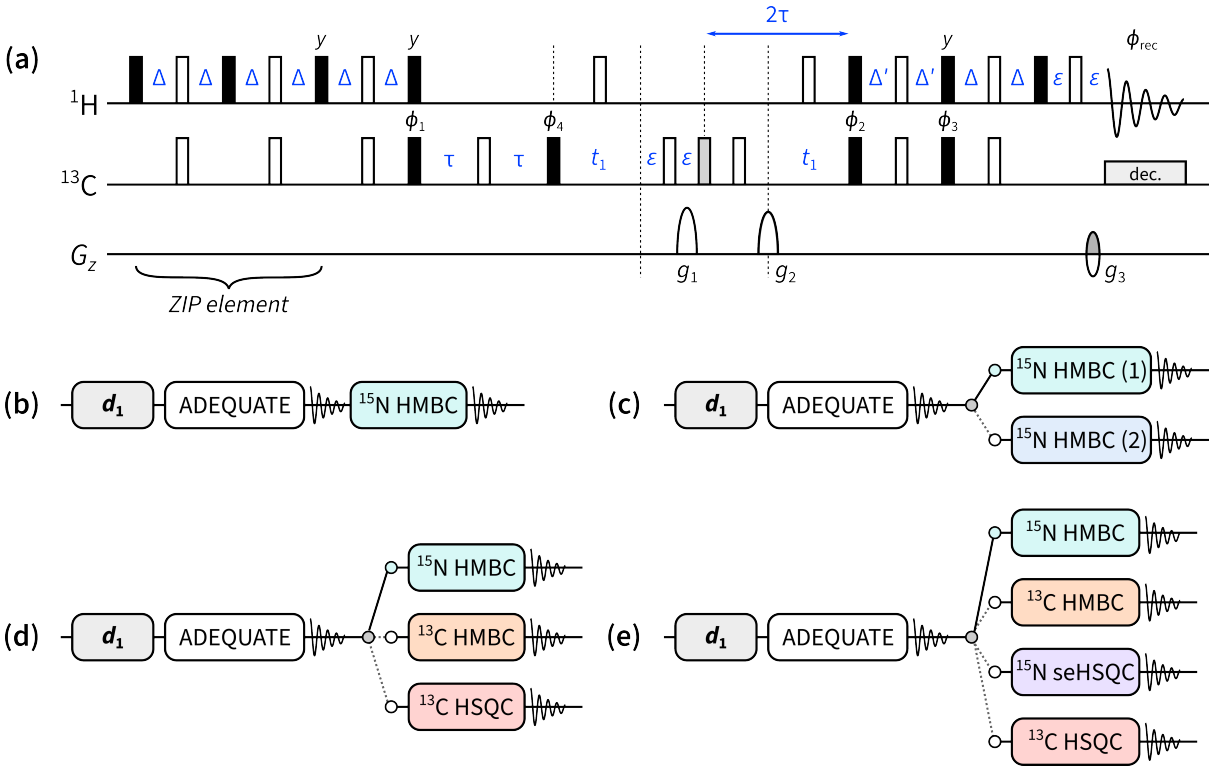

Figure 1: Pulse sequences described in this work. **(a)** ZIP-1,1-ADEQUATE module. Filled and empty bars refer to 90° and 180° pulses respectively; the grey filled bar is a 120° pulse for ^{13}C double-quantum to single-quantum coherence transfer.[21] Pulse and receiver phases are: $\phi_1 = x, -x$; $\phi_2 = 2(x), 2(-x)$; $\phi_3 = 2(y), 2(-y)$; $\phi_4 = 4(x), 4(-x)$; $\phi_{rec} = x, -x, -x, x, -x, x, x, -x$. Delays are set as follows: $\Delta = 1/(4 \cdot {}^1J_{CH})$, $\Delta' = 1/(8 \cdot {}^1J_{CH})$, and $\tau = 1/(4 \cdot {}^1J_{CC})$. ε is the minimum time required for a pulsed field gradient and the following recovery delay. Gradient amplitudes as a percentage of the maximum amplitude are: $g_1 = 78.5\%$, $g_2 = 77.6\%$, and $g_3 = -59\%$. Echo–antiecho selection is achieved by inverting the sign of g_3 as well as the pulse phase ϕ_3. **(b)** NOAH-2 AB_N supersequence. **(c)** NOAH-3 AB_NB_N, where the two ^{15}N HMBC experiments are optimised for two different values of ${}^nJ_{NH}$. **(d)** NOAH-4 AB_NBS. **(e)** NOAH-5 $AB_NBS^+_NS$.

the magnetisation of all other protons (denoted as $^1H^{!C}$) to the equilibrium $+z$ state. This is accomplished by replacing the initial 90° excitation pulse by the *zz*-isotope selective pulse element (ZIP),[23,24] which effects $90°_{-x}$ and $90°_{-y}$ rotations on $^1H^C$ and $^1H^{!C}$ magnetisation respectively. (Other isotope-specific elements such as BANGO[25–27] may also be used here, with similar results generally being obtained.[23]) The ^{15}N HMBC module of choice is a simple magnitude-mode version, with an optional first-order low-pass J-filter. In the NOAH-2 AB_N supersequence (ADEQUATE + ^{15}N HMBC, Figure 1b), this module simply consumes the remaining $^1H^{!C}$ magnetisation which was preserved by the ZIP-ADEQUATE.

3 NOAH-3 AB_NB_N

Although this AB_N sequence performs well on its own (Figure 2), it suffers from the drawback that the ^{15}N HMBC is optimised for one specific value of ${}^nJ_{NH}$. In practice, ${}^nJ_{NH}$ values range from 2–16 Hz; in a

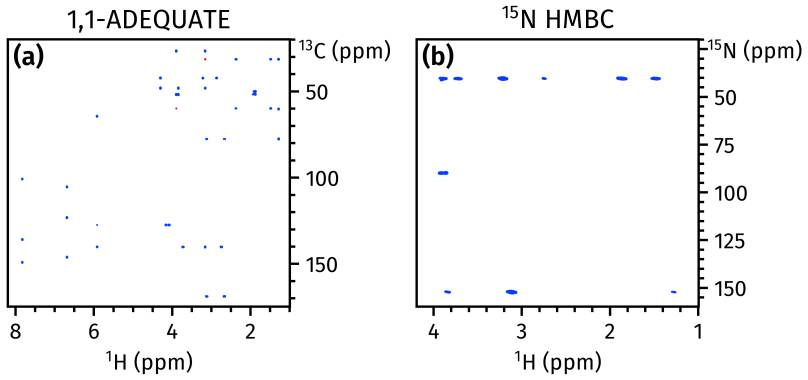

Figure 2: Spectra obtained from the NOAH-2 AB_N supersequence. **(a)** 1,1-ADEQUATE. **(b)** ^{15}N HMBC. Spectra were obtained on a 700 MHz Bruker AV III equipped with a TCI H/C/N cryoprobe; the sample used was 50 mM brucine in $CDCl_3$.

single HMBC experiment, some correlations may therefore be lost due to J-coupling mismatch.

To circumvent this issue, a variety of accordion-type experiments[28–32] have been designed which decrement the J-evolution period in step with t_1, allowing a wider range of couplings to be sampled. Here, we adopt the simpler approach of recording two separate HMBC experiments optimised for different $^{n}J_{NH}$ values. These two HMBC modules cannot be performed *sequentially*, as they both draw on the same $^{1}H^{!C}$ magnetisation; if concatenated 'horizontally' within a supersequence, the second HMBC would suffer from severely decreased sensitivity. However, they can easily be executed in an *interleaved* manner where, after the ADEQUATE module, the two HMBC experiments are alternately acquired.[7] In Figure 1c, this is illustrated by a 'vertical' stacking of the two modules. Thus, after each odd-numbered increment of the ADEQUATE, the first HMBC is acquired; and after each even-numbered increment, the second HMBC is acquired. This means that both HMBC spectra have half the usual number of t_1 increments compared to the ADEQUATE, which is acceptable since the ^{15}N dimension is typically sparse and a high resolution is not required. As can be seen in Figure 3, the two HMBC spectra reveal different sets of correlations.

4 NOAH-4 AB_NBS

In the above AB_NB_N experiment and in previous work,[7] we have shown how two alternating modules can be used to construct parallel supersequences. This concept can naturally be further generalised in order to allow $N \geq 2$ different experiments to be acquired alternately as the second module in the supersequence. These interleaved experiments can be arranged such that they each have lower resolution compared to the first module (as was done in the AB_NB_N experiment), or such that they each have a fewer number of transients. In principle, a similar interleaving may be performed for *all* modules in a supersequence. However, it is important to remember that earlier modules affect the amount of magnetisation passed on to the later modules; thus, it is typically more robust to interleave later modules in a sequence, which avoids discrepancies in data intensity or spectral quality.

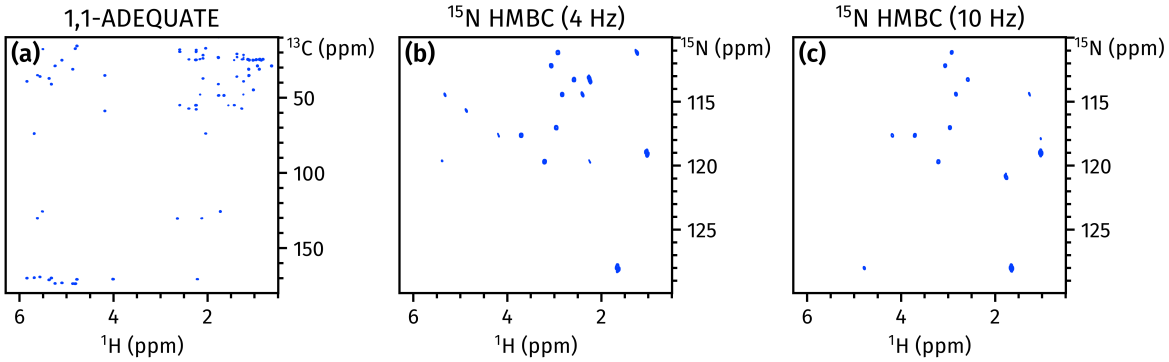

Figure 3: Spectra obtained from the NOAH-3 AB_NB_N supersequence. **(a)** 1,1-ADEQUATE (256 t_1 increments). **(b)** ^{15}N HMBC optimised for $^{n}J_{NH} = 4$ Hz (128 t_1 increments). **(c)** ^{15}N HMBC optimised for $^{n}J_{NH} = 10$ Hz (128 t_1 increments). Spectra were obtained on a 700 MHz Bruker AV III equipped with a TCI H/C/N cryoprobe; the sample used was 50 mM cyclosporin A in C_6D_6.

In the NOAH-4 AB_NBS supersequence (Figure 1d), the ADEQUATE module is followed by one of three choices: a ^{15}N HMBC, a ^{13}C HMBC, or a ^{13}C HSQC. Because these three latter modules do not have the same intrinsic sensitivity, we balance this by allocating a different number of transients to each module. In this specific example, each t_1 increment of the ADEQUATE is recorded a total of $8n$ times (where n is some positive integer); the ^{15}N HMBC $6n$ times; and the ^{13}C HMBC and HSQC n times each. This particular ratio (with $n = 2$) yielded the spectra shown in Figure 4. The pulse programmes provided in the *Supplementary Information* encode these ratios as user-defined constants which may be customised as desired.

One additional feature of the supersequence above concerns the fact that the ^{13}C HSQC module is placed immediately after the ADEQUATE. Both of these modules draw on the same $^{1}H^{C}$ magnetisation pool, and this generally causes the latter module (here HSQC) to suffer from sensitivity losses. Since the HSQC has a much greater intrinsic sensitivity compared to the ADEQUATE, this loss would in fact be tolerable. However, in this experiment, we chose to add a period of isotropic DIPSI-2 mixing[33] immediately before the HSQC module to effect $^{1}H^{!C} \rightarrow {}^{1}H^{C}$ magnetisation transfer, as has previously been done in ASAP[34–37] and NOAH[23] experiments: this replenishes some of the lost $^{1}H^{C}$ magnetisation and leads to greater intensities for the HSQC (Figure S2). This mixing period does not need to be inserted prior to either of the ^{15}N or ^{13}C HMBC modules, as they do not use $^{1}H^{C}$ magnetisation.

The acquisition of the NOAH-4 AB_NBS spectra in Figure 4 took 124 minutes; in contrast, normal acquisition of all four experiments (with the appropriate number of transients) required a total of 223 minutes. As the ADEQUATE is placed first in the supersequence, its sensitivity is almost identical to that of a standalone ADEQUATE; the inclusion of the ZIP element causes only an approximate 5% loss. The ^{15}N and ^{13}C HMBC spectra experience small losses (16–29%) in sensitivity, due to imperfect magnetisation retention by the ADEQUATE module. This is, however, outweighed by the almost twofold time savings provided by concatenation of the modules: if the NOAH supersequence were acquired for as long as

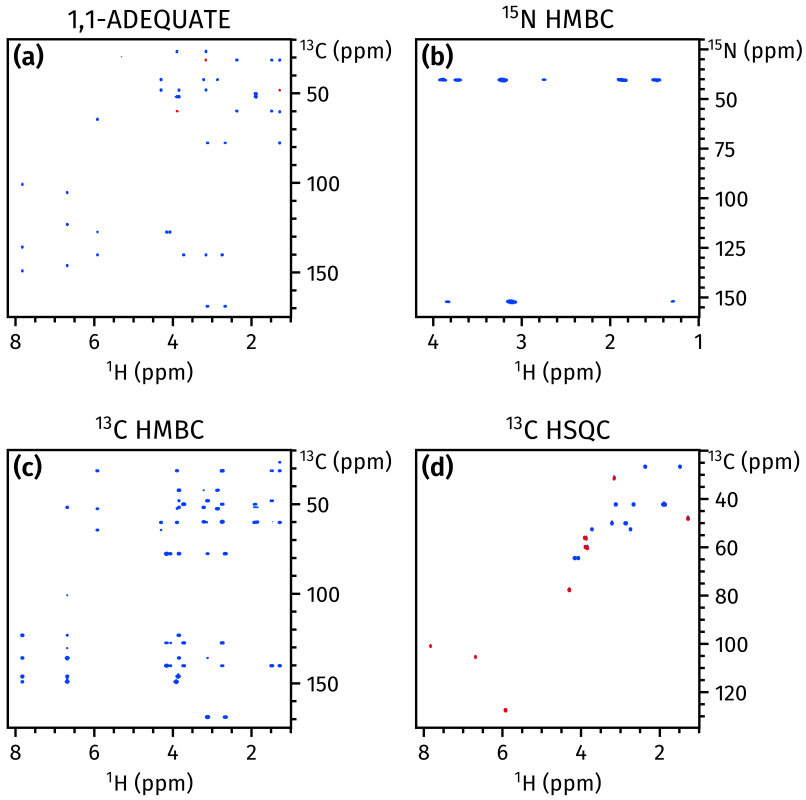

Figure 4: Spectra obtained from the NOAH-4 AB_NBS supersequence. **(a)** 1,1-ADEQUATE (16 transients). **(b)** ^{15}N HMBC (12 transients). **(c)** ^{13}C HMBC (2 transients). **(d)** ^{13}C HSQC (2 transients). Spectra were obtained on a 700 MHz Bruker AV III equipped with a TCI H/C/N cryoprobe; the sample used was 50 mM brucine in $CDCl_3$.

the standalone experiments were, the ^{15}N HMBC spectra would have almost the same SNR, and the ^{13}C HMBC from the NOAH would in fact have a 12% improvement in SNR. Due to the reuse of $^{1}H^{C}$ magnetisation, the HSQC module only retains 29% of its original sensitivity. However, as the HSQC is still two orders of magnitude more sensitive than the ADEQUATE, this decrease is readily tolerated; if necessary, the sensitivity-enhanced HSQC module[23,24,38,39] may also be used in its place.

5 NOAH-5 $AB_NBS^+_NS$

As a final example, we add a further ^{15}N seHSQC module to the above sequence. This is most easily accomplished by simply reducing the number of transients for the ^{15}N HMBC by n and diverting these instead towards a ^{15}N seHSQC, and means that the second slot in the supersequence now alternates between four different experiments (Figure 1e). In principle, the ^{15}N seHSQC uses only $^{1}H^{N}$ magnetisation (i.e. protons directly bonded to ^{15}N), and can simply be added *linearly* as a third module to the supersequence: such an arrangement would maximise its sensitivity as a larger number of transients are collected. However, this would compromise the performance of the other modules, as they must then be modified to preserve the requisite $^{1}H^{N}$ magnetisation: for example, the HMBC modules would need to be

modified to include the *zz*-filter,[5,6] which generally causes 10–20% sensitivity losses. As the ^{15}N seHSQC is a relatively undemanding experiment in terms of sensitivity, it makes more sense to implement it in a 'vertical', interleaved manner. This example especially illustrates how the use of interleaved *and* sequential acquisition leads to much greater flexibility in supersequence design, especially when considering the relative sensitivities of different modules.

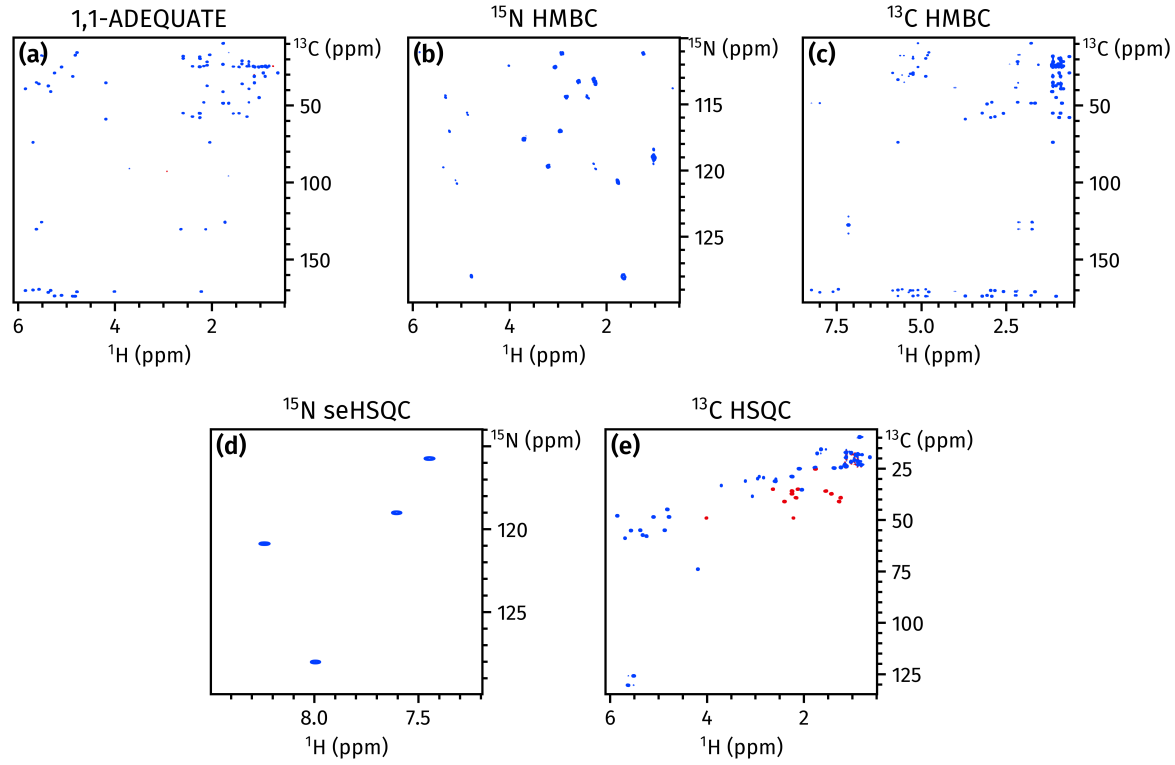

Figure 5: Spectra obtained from the NOAH-5 $AB_NBS^+_NS$ supersequence. **(a)** 1,1-ADEQUATE (16 transients). **(b)** ^{15}N HMBC (10 transients). **(c)** ^{13}C HMBC (2 transients). **(d)** ^{15}N sensitivity-enhanced HSQC (2 transients). **(e)** ^{13}C HSQC (2 transients). Spectra were obtained on a 700 MHz Bruker AV III equipped with a TCI H/C/N cryoprobe; the sample used was 50 mM cyclosporin A in C_6D_6.

The five spectra obtained from this sequence are shown in Figure 5. Collectively, this supersequence provides virtually all heteronuclear correlation data required for structural elucidation or assignment. This is similar in spirit to the PANACEA experiment,[40,41] but yields greater sensitivity as it uses equilibrium ^{1}H magnetisation rather than the low-magnetogyric ratio ^{13}C and ^{15}N nuclei, and does not require multiple-receiver hardware.[4,42] Of course, the ADEQUATE experiment may not be necessary for every novel compound encountered; however, in cases where it *is* needed, the supersequences described here demonstrate that other valuable heteronuclear spectra can also be acquired in a time-efficient manner along with the ADEQUATE.

Furthermore, the heteronuclear spectra collected this way can be processed using indirect covariance processing[43–45] to yield other forms of correlation spectra. For example, the ^{15}N HMBC and ^{13}C HSQC

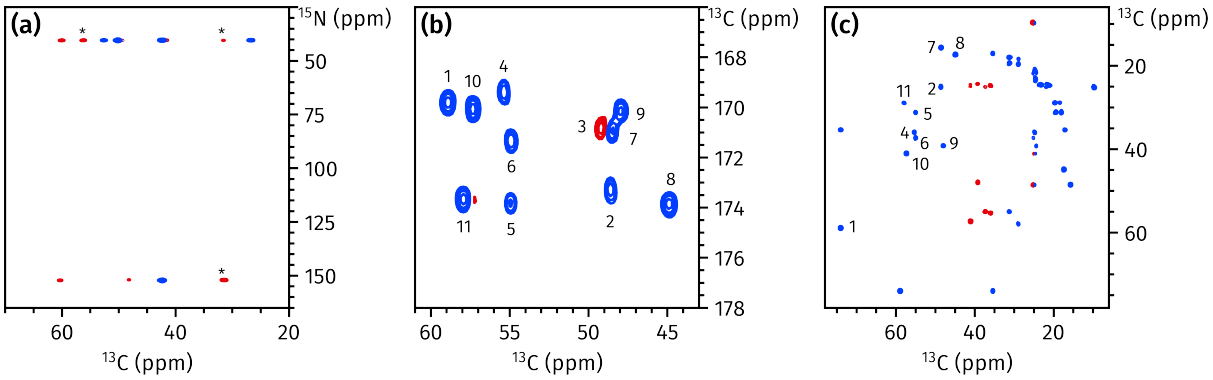

Figure 6: Spectra obtained through indirect covariance processing. In all cases the peak sign indicates carbon multiplicity; this information is contained in the multiplicity-edited ^{13}C HSQC spectrum and arises naturally during covariance processing. **(a)** ^{13}C–^{15}N correlation spectrum (containing both one- and multiple-bond correlations) obtained by processing the brucine ^{15}N HMBC and ^{13}C HSQC spectra (in Figures 4b and 4d) using unsymmetric indirect covariance. Some artefacts (arising from peak overlap in the ^{1}H dimension) are marked with asterisks. **(b–c)** Insets of ^{13}C–^{13}C one-bond correlation spectrum, obtained by processing the cyclosporin ADEQUATE and ^{13}C HSQC spectra (in Figures 5a and 5e) using generalised indirect covariance ($\lambda = 0.5$). The Cα–CO correlations, numbered by residue (see Figure S3), are shown in (b). Sidechain C−C correlations are shown in (c); only peaks corresponding to Cα–Cβ correlations are labelled. The inset in (c) has been further subjected to a sign-preserving symmetrisation procedure, described further in Section S6.

can be used to generate ^{13}C–^{15}N correlation spectra.[46,47] Furthermore, the ^{13}C HSQC and ADEQUATE experiments can be used to create ^{13}C–^{13}C one-bond correlation spectra.[48,49] It should be further emphasised that all of the 'base' spectra used as the inputs here are obtained *in a single measurement* using either the NOAH-4 or NOAH-5 supersequences discussed above. A notable benefit of this is that t_1 for all modules are incremented simultaneously: this minimises the effects of temporal variations such as temperature drift or chemical reactions, which can lead to inaccurate peaks in covariance spectra.

6 Conclusion(ish)

In conclusion, we have demonstrated here how low-sensitivity experiments, such as 1,1-ADEQUATE and ^{15}N HMBC, may be optimally combined in NMR supersequences, leading to substantial reductions in experiment time. Through a generalisation of our previous concept of parallel supersequences, further high-sensitivity modules may be added to the supersequence both 'horizontally' and 'vertically', corresponding respectively to sequential and interleaved acquisition. The spectra thus obtained provide the chemist with far more powerful tools for the characterisation of complex molecules, especially in cases where existing NOAH supersequences do not provide sufficient information for unambiguous assignment.

While the generalised supersequences presented here enable modules to be assembled in almost any imaginable way, their increasing complexity mean that pulse programme construction is more difficult. At present, the GENESIS tool for automatic pulse sequence generation[50] provides only limited options

for parallel supersequences. In particular, it is restricted to only *two* different interleaved modules (as demonstrated in previous work[7]). Different AU programmes are also required to process the data correctly. The pulse sequences and processing scripts used in this work are provided in the Bruker User Library, accessible at https://www.bruker.com/en/services/bruker-user-library.html.

Acknowledgements

We thank Dr Mohammadali Foroozandeh (University of Oxford) for helpful discussions. J.R.J.Y. thanks the Clarendon Fund (University of Oxford) and the EPSRC Centre for Doctoral Training in Synthesis for Biology and Medicine (EP/L015838/1) for a studentship, generously supported by AstraZeneca, Diamond Light Source, Defence Science and Technology Laboratory, Evotec, GlaxoSmithKline, Janssen, Novartis, Pfizer, Syngenta, Takeda, UCB, and Vertex.

References

(1) Findeisen, M.; Berger, S., *50 and More Essential NMR Experiments: A Detailed Guide*; Wiley: Weinheim, 2013.

(2) Claridge, T. D. W., *High-Resolution NMR Techniques in Organic Chemistry*, 3rd ed.; Elsevier: Amsterdam, 2016.

(3) Kupče, Ē.; Claridge, T. D. W. NOAH: NMR Supersequences for Small Molecule Analysis and Structure Elucidation. *Angew. Chem., Int. Ed.* **2017**, *56*, 11779–11783, DOI: 10.1002/anie.201705506.

(4) Kupče, Ē.; Frydman, L.; Webb, A. G.; Yong, J. R. J.; Claridge, T. D. W. Parallel nuclear magnetic resonance spectroscopy. *Nat. Rev. Methods Primers* **2021**, *1*, 27, DOI: 10.1038/s43586-021-00024-3.

(5) Kupče, Ē.; Claridge, T. D. W. Molecular structure from a single NMR supersequence. *Chem. Commun.* **2018**, *54*, 7139–7142, DOI: 10.1039/c8cc03296c.

(6) Kupče, Ē.; Claridge, T. D. W. New NOAH modules for structure elucidation at natural isotopic abundance. *J. Magn. Reson.* **2019**, *307*, 106568, DOI: 10.1016/j.jmr.2019.106568.

(7) Kupče, Ē.; Yong, J. R. J.; Widmalm, G.; Claridge, T. D. W. Parallel NMR Supersequences: Ten Spectra in a Single Measurement. *JACS Au* **2021**, DOI: 10.1021/jacsau.1c00423.

(8) White, K. N.; Amagata, T.; Oliver, A. G.; Tenney, K.; Wenzel, P. J.; Crews, P. Structure Revision of Spiroleucettadine, a Sponge Alkaloid with a Bicyclic Core Meager in H-Atoms. *J. Org. Chem.* **2008**, *73*, 8719–8722, DOI: 10.1021/jo800960w.

(9) Senior, M. M.; Williamson, R. T.; Martin, G. E. Using HMBC and ADEQUATE NMR Data To Define and Differentiate Long-Range Coupling Pathways: Is the Crews Rule Obsolete? *J. Nat. Prod.* **2013**, *76*, 2088–2093, DOI: 10.1021/np400562u.

(10) Buevich, A. V.; Williamson, R. T.; Martin, G. E. NMR Structure Elucidation of Small Organic Molecules and Natural Products: Choosing ADEQUATE vs HMBC. *J. Nat. Prod.* **2014**, *77*, 1942–1947, DOI: 10.1021/np500445s.

(11) Bax, A.; Summers, M. F. Proton and carbon-13 assignments from sensitivity-enhanced detection of heteronuclear multiple-bond connectivity by 2D multiple quantum NMR. *J. Am. Chem. Soc.* **1986**, *108*, 2093–2094, DOI: 10.1021/ja00268a061.

(12) Crouch, R. C.; Llanos, W.; Mehr, K. G.; Hadden, C. E.; Russell, D. J.; Martin, G. E. Applications of cryogenic NMR probe technology to long-range ^{1}H–^{15}N 2D NMR studies at natural abundance. *Magn. Reson. Chem.* **2001**, *39*, 555–558, DOI: 10.1002/mrc.886.

(13) Martin, G. E.; Williams, A. J. Applications of ^{1}H–^{15}N Long-Range Heteronuclear Shift Correlation and ^{15}N NMR in Alkaloid Chemistry. *Annu. Rep. NMR Spectrosc.* **2015**, *84*, 1–76, DOI: 10.1016/bs.arnmr.2014.10.003.

(14) Williamson, R. T.; Buevich, A. V.; Martin, G. E.; Parella, T. LR-HSQMBC: A Sensitive NMR Technique To Probe Very Long-Range Heteronuclear Coupling Pathways. *J. Org. Chem.* **2014**, *79*, 3887–3894, DOI: 10.1021/jo500333u.

(15) Castañar, L.; Saurí, J.; Williamson, R. T.; Virgili, A.; Parella, T. Pure In-Phase Heteronuclear Correlation NMR Experiments. *Angew. Chem., Int. Ed.* **2014**, *53*, 8379–8382, DOI: 10.1002/anie.201404136.

(16) Saurí, J.; Liu, Y.; Parella, T.; Williamson, R. T.; Martin, G. E. Selecting the Most Appropriate NMR Experiment to Access Weak and/or Very Long-Range Heteronuclear Correlations. *J. Nat. Prod.* **2016**, *79*, 1400–1406, DOI: 10.1021/acs.jnatprod.6b00139.

(17) Bax, A.; Freeman, R.; Frenkiel, T. A. An NMR technique for tracing out the carbon skeleton of an organic molecule. *J. Am. Chem. Soc.* **1981**, *103*, 2102–2104, DOI: 10.1021/ja00398a044.

(18) Reif, B.; Köck, M.; Kerssebaum, R.; Kang, H.; Fenical, W.; Griesinger, C. ADEQUATE, a New Set of Experiments to Determine the Constitution of Small Molecules at Natural Abundance. *J. Magn. Reson., Ser. A* **1996**, *118*, 282–285, DOI: 10.1006/jmra.1996.0038.

(19) Martin, G. E. Using 1,1- and 1,*n*-ADEQUATE 2D NMR Data in Structure Elucidation Protocols. *Annu. Rep. NMR Spectrosc.* **2011**, *74*, 215–291, DOI: 10.1016/B978-0-08-097072-1.00005-4.

(20) Rao Kakita, V. M.; Hosur, R. V. All-in-one NMR spectroscopy of small organic molecules: complete chemical shift assignment from a single NMR experiment. *RSC Adv.* **2020**, *10*, 21174–21179, DOI: 10.1039/d0ra03417g.

(21) Mareci, T. H.; Freeman, R. Echoes and antiechoes in coherence transfer NMR: Determining the signs of double-quantum frequencies. *J. Magn. Reson.* **1982**, *48*, 158–163, DOI: 10.1016/0022-2364(82)90250-5.

(22) Orts, J.; Gossert, A. D. Structure determination of protein-ligand complexes by NMR in solution. *Methods* **2018**, *138-139*, 3–25, DOI: 10.1016/j.ymeth.2018.01.019.

(23) Yong, J. R. J.; Hansen, A. L.; Kupče, Ē.; Claridge, T. D. W. Increasing sensitivity and versatility in NMR supersequences with new HSQC-based modules. *J. Magn. Reson.* **2021**, *329*, 107027, DOI: 10.1016/j.jmr.2021.107027.

(24) Hansen, A. L.; Kupče, Ē.; Li, D.-W.; Bruschweiler-Li, L.; Wang, C.; Brüschweiler, R. 2D NMR-Based Metabolomics with HSQC/TOCSY NOAH Supersequences. *Anal. Chem.* **2021**, *93*, 6112–6119, DOI: 10.1021/acs.analchem.0c05205.

(25) Sørensen, O. W. Selective Rotations Using Non-Selective Pulses and Heteronuclear Couplings. *Bull. Magn. Reson.* **1994**, *16*, 49–53.

(26) Nagy, T. M.; Gyöngyösi, T.; Kövér, K. E.; Sørensen, O. W. BANGO SEA XLOC/HMBC–H2OBC: complete heteronuclear correlation within minutes from one NMR pulse sequence. *Chem. Commun.* **2019**, *55*, 12208–12211, DOI: 10.1039/c9cc06253j.

(27) Nagy, T. M.; Kövér, K. E.; Sørensen, O. W. NORD: NO Relaxation Delay NMR Spectroscopy. *Angew. Chem., Int. Ed.* **2021**, *60*, 13587–13590, DOI: 10.1002/anie.202102487.

(28) Wagner, R.; Berger, S. ACCORD-HMBC: a superior technique for structural elucidation. *Magn. Reson. Chem.* **1998**, *36*, S44–S46, DOI: 10.1002/(sici)1097-458x(199806)36:13<s44::aid-omr281>3.0.co;2-q.

(29) Martin, G. E.; Hadden, C. E.; Crouch, R. C.; Krishnamurthy, V. V. ACCORD-HMBC: advantages and disadvantages of static versus accordion excitation. *Magn. Reson. Chem.* **1999**, *37*, 517–528, DOI: 10.1002/(sici)1097-458x(199908)37:8<517::aid-mrc501>3.0.co;2-w.

(30) Hadden, C. E.; Martin, G. E.; Krishnamurthy, V. V. Improved Performance Accordion Heteronuclear Multiple-Bond Correlation Spectroscopy—IMPEACH-MBC. *J. Magn. Reson.* **1999**, *140*, 274–280, DOI: 10.1006/jmre.1999.1840.

(31) Martin, G. E.; Hadden, C. E. Application of accordion excitation in ^{1}H–^{15}N long-range heteronuclear shift correlation experiments at natural abundance. *Magn. Reson. Chem.* **2000**, *38*, 251–256, DOI: 10.1002/(sici)1097-458x(200004)38:4<251::aid-mrc625>3.0.co;2-j.

(32) Hadden, C. E.; Martin, G. E.; Krishnamurthy, V. V. Constant time inverse-detection gradient accordion rescaled heteronuclear multiple bond correlation spectroscopy: CIGAR-HMBC. *Magn. Reson. Chem.* **2000**, *38*, 143–147, DOI: 10.1002/(sici)1097-458x(200002)38:2<143::aid-mrc624>3.0.co;2-s.

(33) Shaka, A. J.; Lee, C. J.; Pines, A. Iterative schemes for bilinear operators; application to spin decoupling. *J. Magn. Reson.* **1988**, *77*, 274–293, DOI: 10.1016/0022-2364(88)90178-3.

(34) Schulze-Sünninghausen, D.; Becker, J.; Luy, B. Rapid Heteronuclear Single Quantum Correlation NMR Spectra at Natural Abundance. *J. Am. Chem. Soc.* **2014**, *136*, 1242–1245, DOI: 10.1021/ja411588d.

(35) Schulze-Sünninghausen, D.; Becker, J.; Koos, M. R. M.; Luy, B. Improvements, extensions, and practical aspects of rapid ASAP-HSQC and ALSOFAST-HSQC pulse sequences for studying small molecules at natural abundance. *J. Magn. Reson.* **2017**, *281*, 151–161, DOI: 10.1016/j.jmr.2017.05.012.

(36) Koos, M. R. M.; Luy, B. Polarization recovery during ASAP and SOFAST/ALSOFAST-type experiments. *J. Magn. Reson.* **2019**, *300*, 61–75, DOI: 10.1016/j.jmr.2018.12.014.

(37) Becker, J.; Koos, M. R. M.; Schulze-Sünninghausen, D.; Luy, B. ASAP-HSQC-TOCSY for fast spin system identification and extraction of long-range couplings. *J. Magn. Reson.* **2019**, *300*, 76–83, DOI: 10.1016/j.jmr.2018.12.021.

(38) Palmer, A. G.; Cavanagh, J.; Wright, P. E.; Rance, M. Sensitivity improvement in proton-detected two-dimensional heteronuclear correlation NMR spectroscopy. *J. Magn. Reson.* **1991**, *93*, 151–170, DOI: 10.1016/0022-2364(91)90036-S.

(39) Kay, L.; Keifer, P.; Saarinen, T. Pure absorption gradient enhanced heteronuclear single quantum correlation spectroscopy with improved sensitivity. *J. Am. Chem. Soc.* **1992**, *114*, 10663–10665, DOI: 10.1021/ja00052a088.

(40) Kupče, Ē.; Freeman, R. Molecular Structure from a Single NMR Experiment. *J. Am. Chem. Soc.* **2008**, *130*, 10788–10792, DOI: 10.1021/ja8036492.

(41) Kupče, Ē.; Freeman, R. Molecular structure from a single NMR sequence (fast-PANACEA). *J. Magn. Reson.* **2010**, *206*, 147–153, DOI: 10.1016/j.jmr.2010.06.018.

(42) Kupče, Ē.; Mote, K. R.; Webb, A.; Madhu, P. K.; Claridge, T. D. W. Multiplexing experiments in NMR and multi-nuclear MRI. *Prog. Nucl. Magn. Reson. Spectrosc.* **2021**, *124-125*, 1–56, DOI: 10.1016/j.pnmrs.2021.03.001.

(43) Zhang, F.; Brüschweiler, R. Indirect Covariance NMR Spectroscopy. *J. Am. Chem. Soc.* **2004**, *126*, 13180–13181, DOI: 10.1021/ja047241h.

(44) Snyder, D. A.; Brüschweiler, R. Generalized Indirect Covariance NMR Formalism for Establishment of Multidimensional Spin Correlations. *J. Phys. Chem. A* **2009**, *113*, 12898–12903, DOI: 10.1021/jp9070168.

(45) Jaeger, M.; Aspers, R. L. E. G. Covariance NMR and Small Molecule Applications. *Annu. Rep. NMR Spectrosc.* **2014**, *83*, 271–349, DOI: 10.1016/B978-0-12-800183-7.00005-8.

(46) Martin, G. E.; Hilton, B. D.; Irish, P. A.; Blinov, K. A.; Williams, A. J. ^{13}C–^{15}N connectivity networks via unsymmetrical indirect covariance processing of ^{1}H–^{13}C HSQC and ^{1}H–^{15}N IMPEACH spectra. *Journal of Heterocyclic Chemistry* **2007**, *44*, 1219–1222, DOI: 10.1002/jhet.5570440541.

(47) Martin, G. E.; Irish, P. A.; Hilton, B. D.; Blinov, K. A.; Williams, A. J. Utilizing unsymmetrical indirect covariance processing to define ^{15}N–^{13}C connectivity networks. *Magn. Reson. Chem.* **2007**, *45*, 624–627, DOI: 10.1002/mrc.2029.

(48) Martin, G. E.; Hilton, B. D.; Blinov, K. A. HSQC-ADEQUATE correlation: a new paradigm for establishing a molecular skeleton. *Magn. Reson. Chem.* **2011**, *49*, 248–252, DOI: 10.1002/mrc.2743.

(49) Martin, G. E.; Hilton, B. D.; Willcott III, M. R.; Blinov, K. A. HSQC-ADEQUATE: an investigation of data requirements. *Magn. Reson. Chem.* **2011**, *49*, 350–357, DOI: 10.1002/mrc.2757.

(50) Yong, J. R. J.; Kupče, Ē.; Claridge, T. D. W. Modular Pulse Program Generation for NMR Supersequences. *Anal. Chem.* **2022**, *94*, 2271–2278, DOI: 10.1021/acs.analchem.1c04964.

Supporting Information

for

Uniting Low- and High-Sensitivity Experiments through Generalised NMR Supersequences

Jonathan R. J. Yong,[1] Ēriks Kupče,[2] Tim D. W. Claridge[1,*]

[1] *Chemistry Research Laboratory, Department of Chemistry, University of Oxford, Mansfield Road, Oxford, OX1 3TA, United Kingdom*

[2] *Bruker UK Ltd, R&D, Coventry CV4 9GH, United Kingdom*

[*] tim.claridge@chem.ox.ac.uk

Contents

S1 Pulse programme description

With a more detailed diagram & explanation

S2 Pulse programme setup

For ABBS, the thought process is generally as follows:

- Decide on number of t_1 increments for each module (we call this N_1). This is determined by desired resolution in indirect dimension. Say 256.
- Decide on NS for each module. NS for ADEQUATE must be equal to sum of NS for all other modules.
- Determine the gcd of the separate NS's (for example, gcd(16, 12, 2, 2) = 2). Set the TopSpin parameter `NS` as this value. Make sure this is at least 2 as this determines the minimum phase cycle
- Set (`cnst51`, `cnst52`, `cnst53`, `cnst54`) = NS's divided through by their gcd (so 8, 6, 1, 1). In practice the last of these is automatically calculated, so it doesn't have to be set.
- Set `NBL` = 2 since there are only really two 'horizontally' combined modules.
- Set TopSpin `TD1` parameter to be $N_1 \times$ `NBL` $\times$ `cnst51`. In this case, $256 \times 2 \times 8 = 4096$.

Should note here that previous parallel supersequences[1] essentially follow the same idea but with two threads. The sequences don't explicitly use the `cnst` parameters as shown above, but in practice they behave exactly as if `cnst51` = 2 and `cnst52` = `cnst53` = 1.

This observation, in principle, should open up a 'path' to generalising the GENESIS algorithm—but I need time to do it. Providing a GUI is also problematic. (I have some *ideas* about the desired UI, but actually *implementing* it is another matter…)

S3 Spectra that didn't make it into the main text

(We should move some figures from the main text to here—the only question is which ones?

Since the ^{1}H–^{1}H NOESY uses the same ^{1}H$^{!C}$ magnetisation as ^{13}C HMBC so can be directly substituted in its place, leading to a NOAH-4 AB$_N$NS supersequence (Figure S1). This not only provides a wealth of through-bond correlations which aid in eludicating molecular constitution, but also furnishes through-space correlations for the determination of configuration or conformation.

One *actual* problem here is the receiver gain. For ABBS I had RG = 2050, but for this I had to set RG = 29(!!).

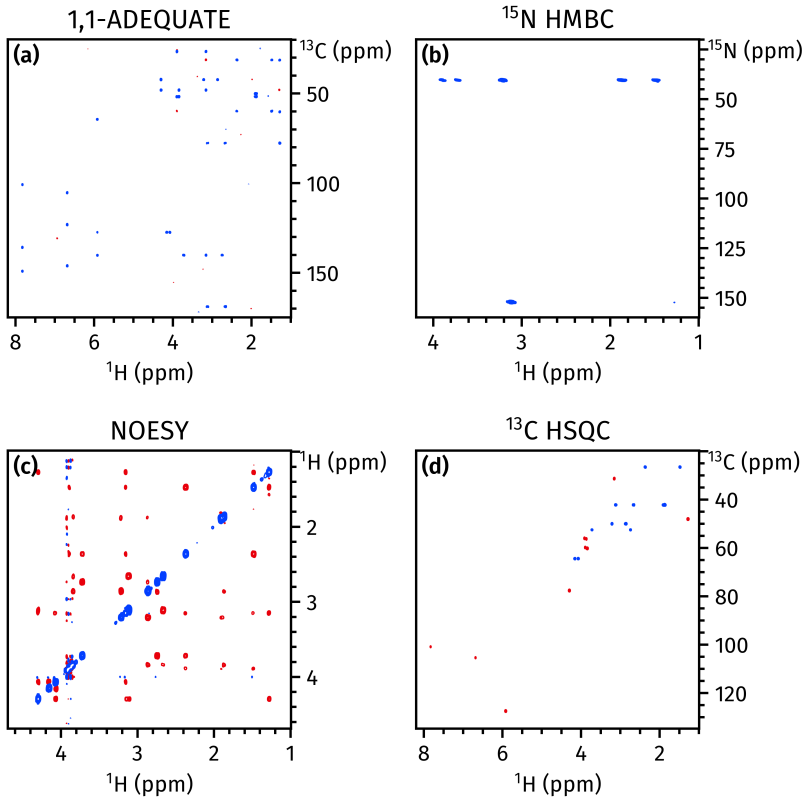

Figure S1: Spectra obtained from the NOAH-4 AB_NNS supersequence. **(a)** 1,1-ADEQUATE (16 transients). **(b)** ^{15}N HMBC (12 transients). **(c)** NOESY (2 transients, 800 ms mixing time). **(d)** ^{13}C HSQC (2 transients). Spectra were obtained on a 700 MHz Bruker AV III equipped with a TCI H/C/N cryoprobe; the sample used was 50 mM brucine in $CDCl_3$.

S4 ABBS comparison with and without DIPSI

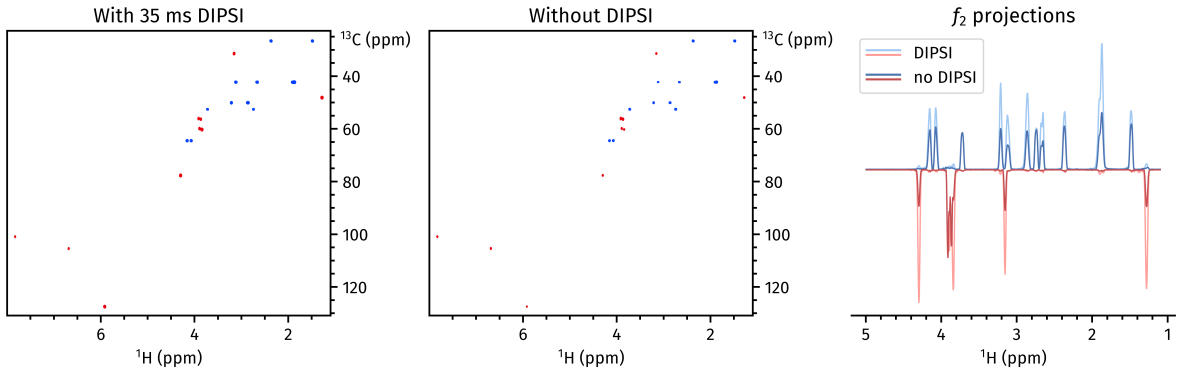

Figure S2: ^{13}C HSQC spectra obtained from the NOAH-4 AB_NBS experiment (Figure 1d). **(a)** Without DIPSI mixing between the ADEQUATE and ^{13}C HSQC modules. **(b)** With 35 ms DIPSI mixing between the ADEQUATE and ^{13}C HSQC modules (this spectrum is the same as in Figure 4d). **(c)** Projections of the spectra in (a) and (b) onto the f_2 axis. Spectra were obtained on a 700 MHz Bruker AV III equipped with a TCI H/C/N cryoprobe; the sample used was 50 mM brucine in $CDCl_3$.

The average signal enhancement across all peaks is 88% (Figure S2).

Similar to results seen previously[2]

S5 Cyclosporin structure

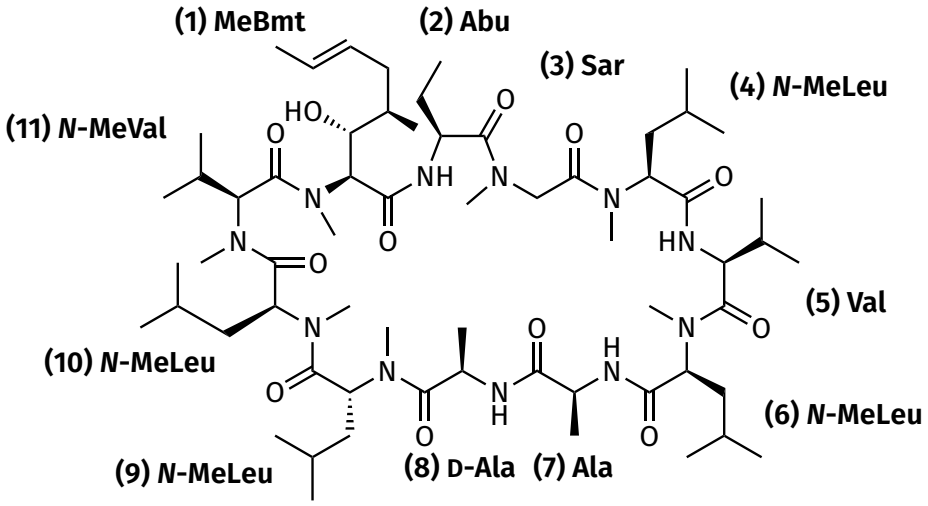

Figure S3: Structure of cyclosporin with residues numbered.

S6 Symmetrisation procedure

In Figure 6c, the ^{13}C–^{13}C one-bond covariance spectrum has been subjected to a sign-preserving symmetrisation procedure. This is defined by replacing the intensity at each point $p(\Omega_1, \Omega_2)$ by

$$p(\Omega_1, \Omega_2) \rightarrow \operatorname{sgn}[p(\Omega_1, \Omega_2)] \cdot \min\{|p(\Omega_1, \Omega_2)|, |p(\Omega_2, \Omega_1)|\}. \quad (1)$$

Here, sgn p refers to the sign of p, or equivalently $p/|p|$ (for $p \neq 0$). The sgn p term ensures that the *sign* of each peak (and hence multiplicity information) is preserved, but the (absolute) intensities are symmetrised about the main diagonal, which suppresses artefactual responses arising from coincidental peak overlap.

It should be noted that such a procedure can only be safely carried out where peaks on both sides of the diagonals are expected to be seen. For a *true* ^{13}C–^{13}C correlation spectrum, this would be the case for all pairs of ^{13}C nuclei. However, the covariance spectrum shown in Figures 6b and 6cdoes not satisfy this: peaks at (Ω_1, Ω_2) are only observed if the carbon at Ω_2 is bonded to at least one proton. Thus, if the symmetrisation procedure is applied across the entire spectrum, correlations between quaternary and non-quaternary carbons (such as those in Figure 6b) will be lost. However, in the case of Figure 6c, the alkyl region of cyclosporin does not contain any quaternary carbons, allowing the symmetrisation can be safely carried out.

References

(1) Kupče, Ē.; Yong, J. R. J.; Widmalm, G.; Claridge, T. D. W. Parallel NMR Supersequences: Ten Spectra in a Single Measurement. *JACS Au* **2021**, DOI: 10.1021/jacsau.1c00423.

(2) Yong, J. R. J.; Hansen, A. L.; Kupče, Ē.; Claridge, T. D. W. Increasing sensitivity and versatility in NMR supersequences with new HSQC-based modules. *J. Magn. Reson.* **2021**, *329*, 107027, DOI: 10.1016/j.jmr.2021.107027.